J. Indian Chem. Soc.,
Vol. 96, March 2019, pp. 385-390

Surface morphological characterization of hydrogenated diamond-like carbon and surface modified hydrogenated diamond-like carbon by scanning probe microscope

Hari Shankar Biswas

Department of Chemistry, Surendranath College, Kolkata-700 009, India

E-mail: harishankarb7@gmail.com

Manuscript received online 02 February 2019, accepted 11 March 2019

Seven sample of hydrogenated diamond-like carbon (HDLC) films onto Si (1 0 0) substrate at room temperature using biased enhanced nucleation (BEN) technique in the reactive gas-plasma process (RGPP) under varying ratio of flow rates of H_2 and CH_4. Thus the as-prepared HDLC samples are named as S44, S42, S40, S38, S36, S34, and S32. Atomic Force Microscopy (AFM) has the unique capability of probing the nanoscale surface morphological properties of carbon base materials and biological systems. In this paper the force of attraction in nano Newton (nN) unit and surface roughness in nm unit of the HDLCs and surface modified HDLCs sample by Bovine Serum Albumin (BSA) was measured quantitatively by AFM. It is seen that a clear correlation with force of attraction with hydrogen content in the surface, roughness of the surface and presence of bimolecules in the surface.

Keywords: Hydrogenated diamond, AFM, force of attraction, surface roughness.

Introduction

Hydrogenated diamond-like carbon (HDLC) has an atomically-smooth surface that can be deposited on high-surface area substrate and functionalized with reactive chemical groups, providing an ideal substrate for protein immobilization[1,2]. Atomic force microscopy (AFM) is a powerful surface morphology characterization technique[3,4]. The use of atomic force microscopy (AFM) to probe the distance dependent forces between various materials[5,6] separated by air, liquid, and vacuum have recently gained much interest. AFM is a three-dimensional surface topography imaging technique whereas STM[4,7] provides pictures of atoms on surfaces. STM and AFM provide sub-nanometer resolution in all three dimensions, but because a voltage is exerted onto the sample in STM, the technique is limited to conducting and semiconducting samples. On account of the low conductance of most amorphous or nanocrystalline carbon films, AFM is more widely used. AFM measures the local attractive or repulsive forces between the probe tip and sample surface[8]. An AFM instrument uses a micro-machined cantilever with a tip at the end to sense the sample surface. As the tip is repelled by or attracted to the surface[9], the cantilever beam deflects. The magnitude of the deflection is captured by a laser that reflects at an oblique angle from the very end of the cantilever. As the tip is rastered over the sample, the vertical deflection are recorded and displayed to produce an AFM image. In addition to reconstructing the topography of the surface, the AFM tip can be used to measure at the nanoscale additional surface properties, such as elasticity, hardness or adhesion[6,8]. AFM can achieve a resolution of 0.01 nm, and unlike electron microscopes, can image samples in air or liquids. With regard to the morphology[10] of amorphous carbon and nanocrystalline carbon films, the application is quite straightforward.

Preparation of HDLC thin film deposited on Si (1 0 0) wafer:

A straight forward synthesis of HDLC by the low pressure biased enhanced nucleation (BEN) method at room temperature in an asymmetrically capacitively RF (13.56 MHz) coupled device, involves two steps: (1) etching of mirror polished Si (1 0 0) substrate of 10 mm diameter for 15 min in a pure hydrogen (flow rate ~500 sccm) plasma, at a pressure of 0.190 mbar, produced by 30 Watt RF power producing dc self negative bias (~–200 V), to remove oxide layer from the surface of Si (1 0 0) and (2) *in situ* BEN process using He (flow rate ~1500 sccm) plasma produced by 50 Watt RF power producing dc self negative bias (~–200 V), with H_2 (flow rate ~500 sccm) and CH_4 (flow rate ~50, 60, 70, 80, 90, 100, 110 sccm) gases at a total pressure of 0.756 mbar and at substrate temperature ~14°C, for 30 min deposition time[1].

Experimental

A schematic diagram shows SPM (AFM/STM) instrumental technique used in the measurement of surface morphology, force-distance curves for HDLC samples for the present works is shown in Fig. 1.

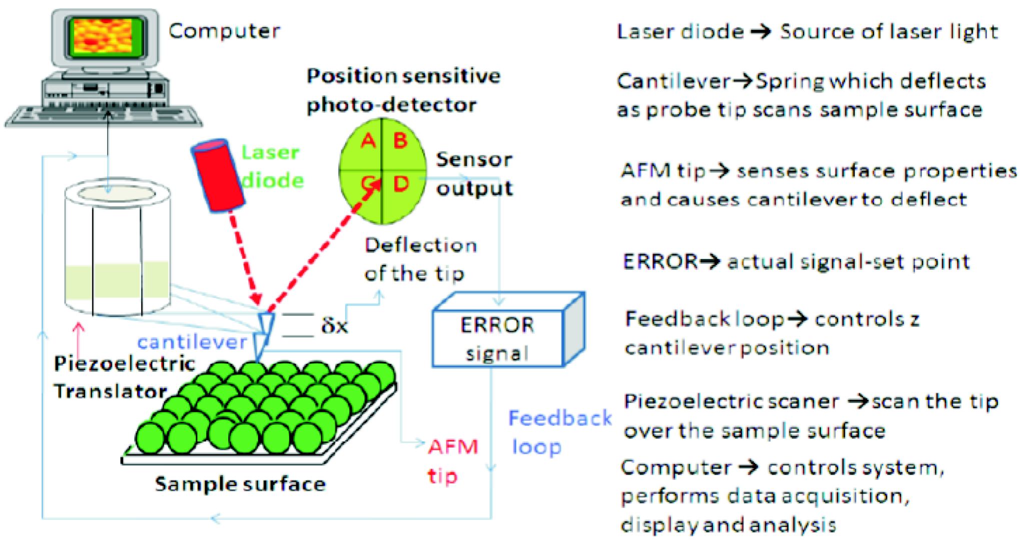

Fig. 1. Schematic diagram of working principle of SPM.

We have demonstrated earlier[1] protein immobilization method onto HDLC surface via L-Dopa linker (D-HDLC) having high loading capacity of proteins with no conformal change and having covalent interaction. Now if conformation of BSA protein in BD-HDLC remains intact then force of attraction of the modified surface will be changed. We have taken the force-distance curves[11] using Si_3N_4 cantilever and Fig. 2 shows a typical AFM deflection (*d*) versus displacement (*h*) curve for freshly clean sample surface and modified sample surface and Si_3N_4 tip of spring constant about (0.765 N/m) in air. AFM images of HDLC in non-contact mode with different scan size were taken and calculated the value of the roughness of the surfaces shown in Table 1.

Results and discussion

The interested results are that the series of our samples numbers S44 to S32, silicon wafer (100), L-DOPA modified HDLC (D-HDLC) and BSA modified HDLC (BD-HDLC) the force between silicon nitride and sample are shown by Fig. 2. It is seen that with the samples number the force of attraction (in nN) are increases. With the increase of methane content the percent of hydrogen increase and number density also increase and roughness of the sample increases. Though the Fig. 2 represented force of attraction is not uniform but their magnitude is uniform. The polarity of the sample decreases and with this force of attraction between sample and Si_3N_4 tip increases[12]. The Fig. 3 represents the 3D AFM images of HDLC surfaces with roughness values range from 0.2 nm to ~0.01 nm, indicating nature of the surface to be continuous, nonporous and smooth. The force-distance curves using Si_3N_4 cantilever have been taken by AFM to probe[13,14] the distance dependent forces[15,12] between Si_3N_4 and HDLC surface separated by air.

Fig. 2 represent a typical force distance curves of HDLC samples: S32, S34, S36, S38, S40, S42, S44, and S32 sample modified by DOPA (D-HDLC) and BSA (BD-HDLC)

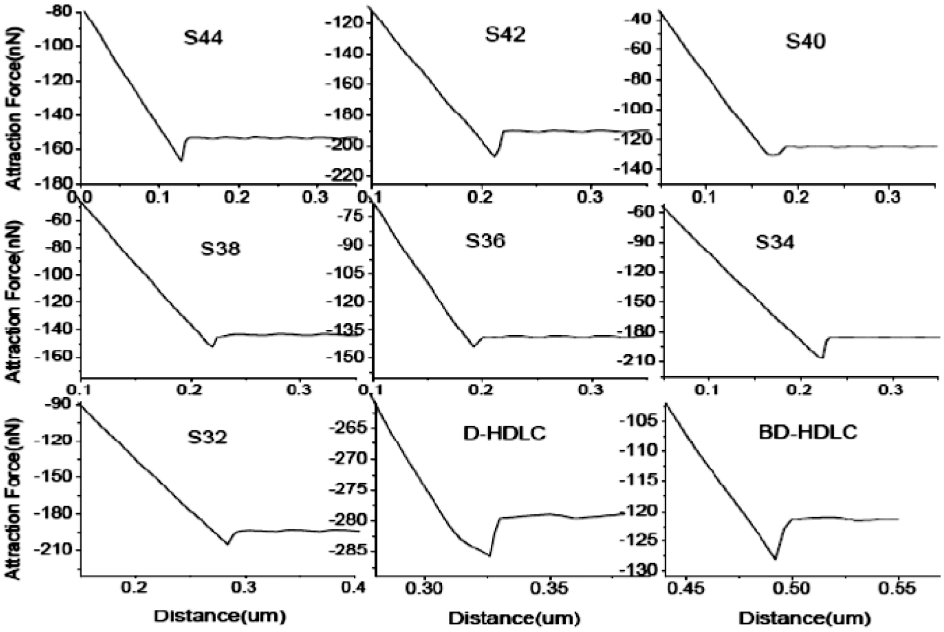

Fig. 2. Typical force distance curves of HDLC samples: S32, S34, S36, S38, S40, S42, S44, and S32 sample modified by DOPA (D-HDLC) and BSA (BD-HDLC) respectively using Si_3N_4 tip of spring constant about (0.765 N/m) in air.

Table 1. Comparative study surface roughness and force of attraction in nm and nN respectively

HDLC sample	F (nN)	Surface roughness by AFM (nm)
S44	1.38±0.25	~0.15
S42	1.47±0.30	~0.12
S40	1.64±0.17	~0.07
S38	1.73±0.30	~0.07
S36	1.74±0.26	~0.05
S34	2.41±0.32	~0.04
S32	1.92±0.18	~0.01
D-HDLC	6.17±0.11	~0.30
BD-HDLC	5.03±0.23	~0.51

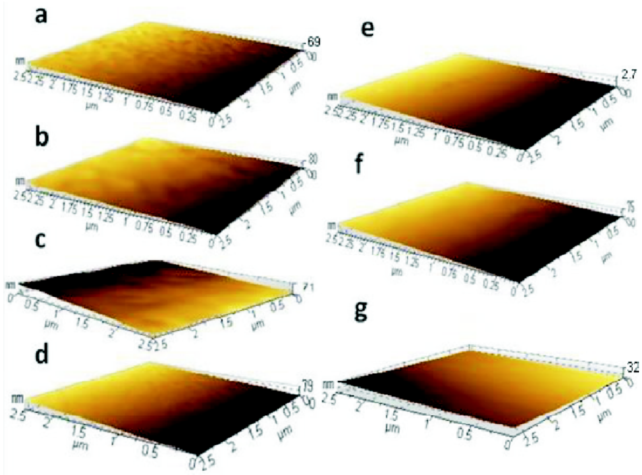

Fig. 3. AFM images of HDLC in non-contact mode with scan size 2.5 µm by 2.5 µm: (a) S44, (b) S42, (c) S40, (d) S38, (e) S36, (f) S34, (g) S32.

respectively using Si_3N_4 tip of spring constant about (0.765 N/m) in air. The force of attraction of (D-HDLC) and BSA (BD-HDLC) is very high compare to Si (1 0 0) and HDLC samples due to covalent binding and aggregation of L-Dopa and BSA protein with HDLC[1].

The Fig. 4 represents the typical 2D and 3D AFM images of S44 HDLC surfaces with roughness value 0.145 nm and undulating surface topography through the indicating line.

The Fig. 5 represents the typical 2D and 3D AFM images of S36 HDLC surfaces with roughness value 0.0716 nm and undulating surface topography through the indicating line on the surface.

The Fig. 6 represents the typical 2D and 3D AFM images of S32 HDLC surfaces with roughness value 0.0145 nm and

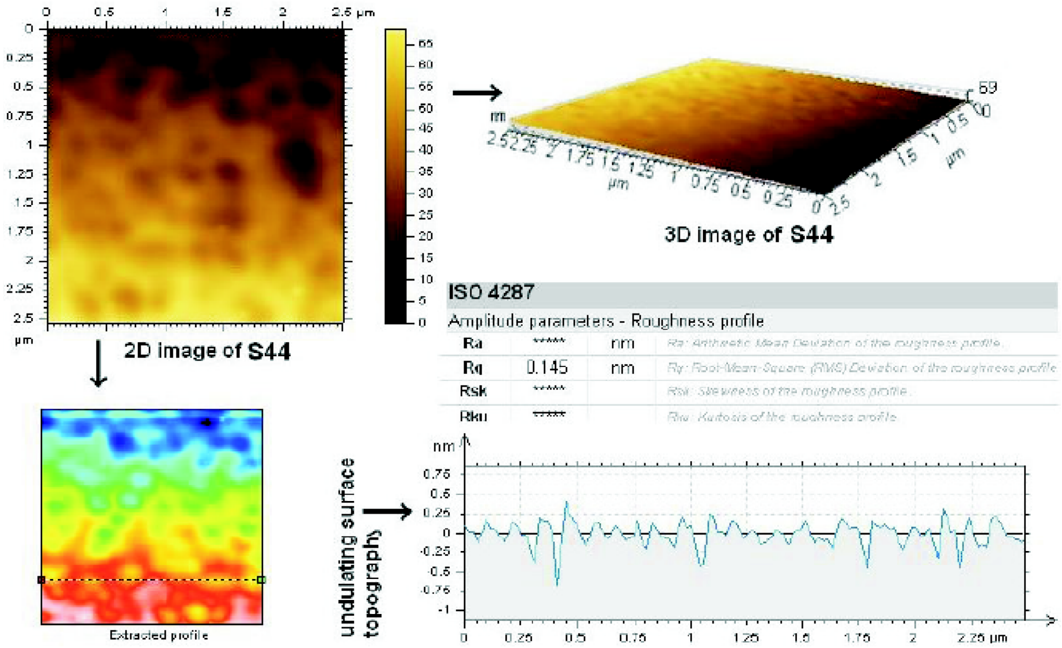

Fig. 4. Typical 2D and 3D AFM images of S44 HDLC sample with roughness value.

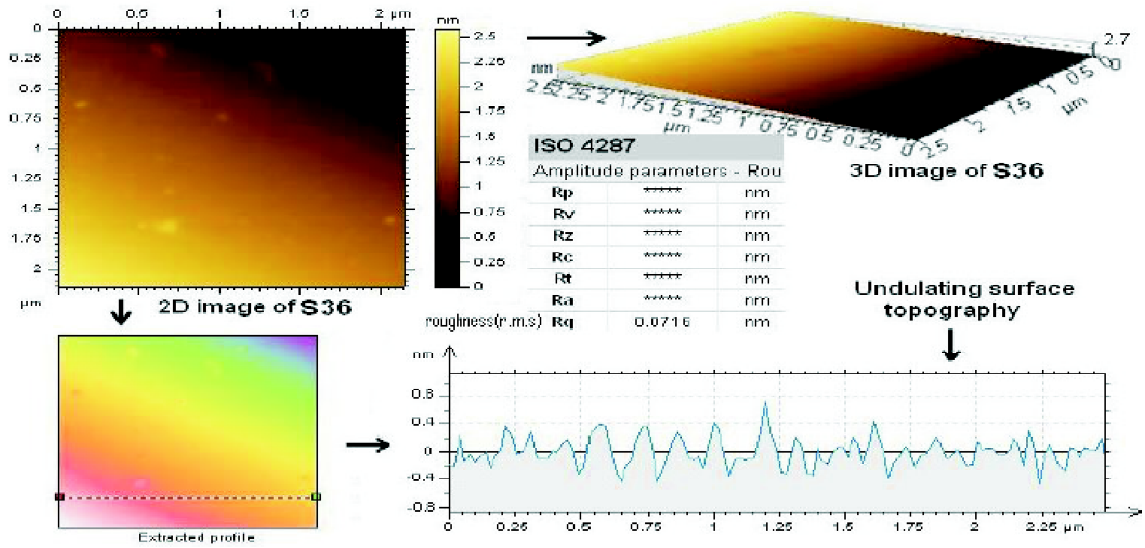

Fig. 5. Typical 2D and 3D AFM image of S36 HDLC surface.

undulating surface topography through the indicating line.

The Fig. 7 represents the typical 2D AFM images of BD-HDLC surfaces with roughness value 0.51 nm and undulating surface topography through the indicating line.

It is seen from Table 1 with the increase of surface roughness force of attraction gradually increases due to increase of number density due to increases of hydrogen incorporation and surface modification by biomolecules.

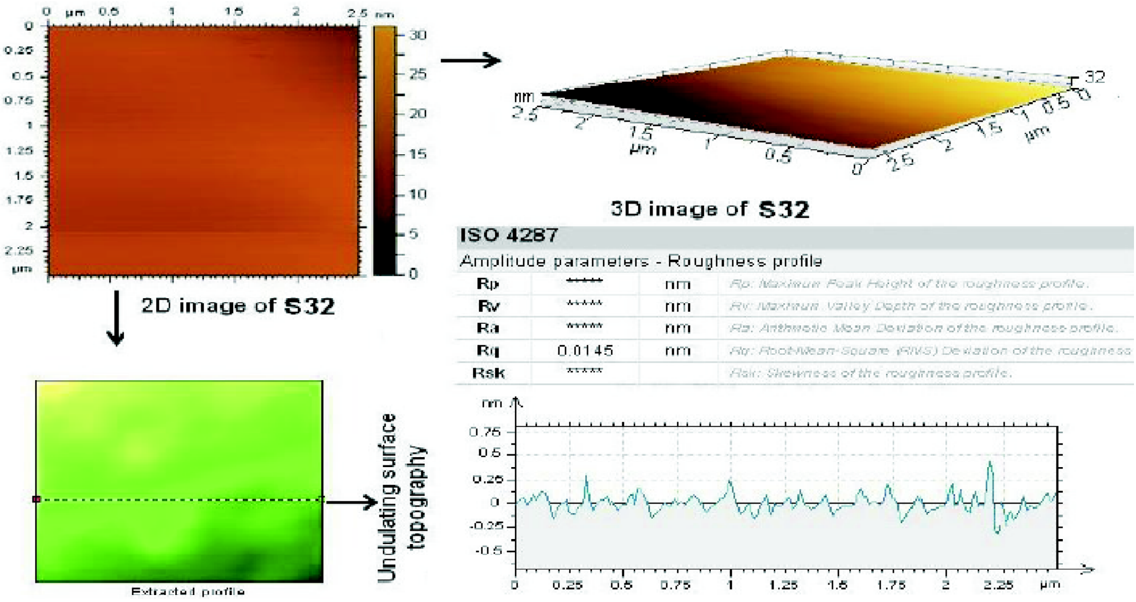

Fig. 6. Typical 2D and 3D AFM image of S32 HDLC sample with roughness value.

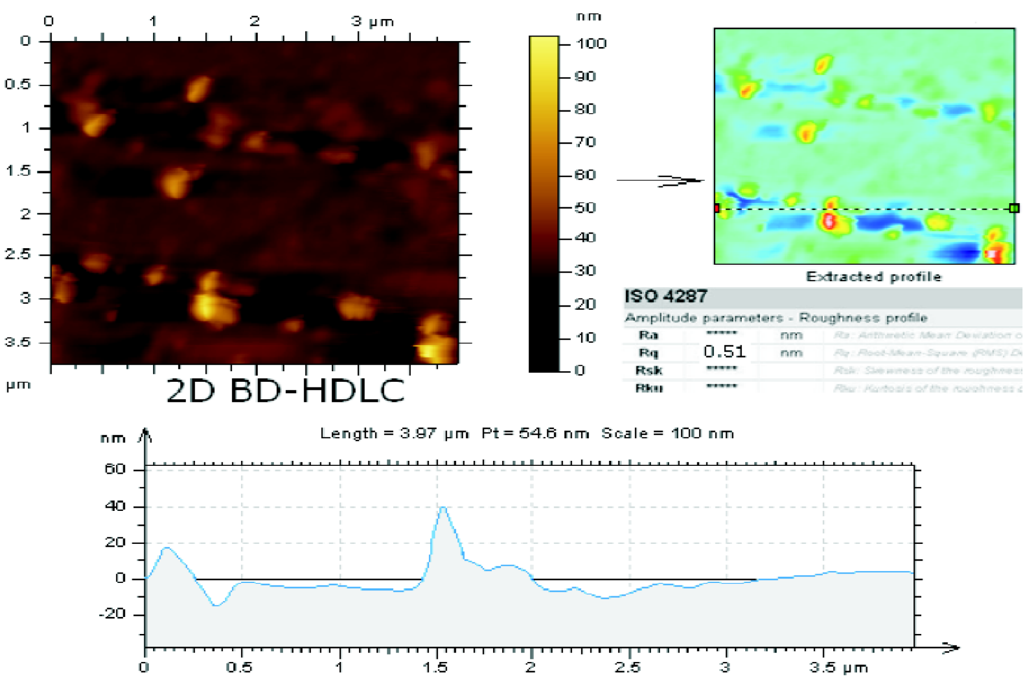

Fig. 7. Typical 2D AFM image of BD-HDLC sample with roughness value.

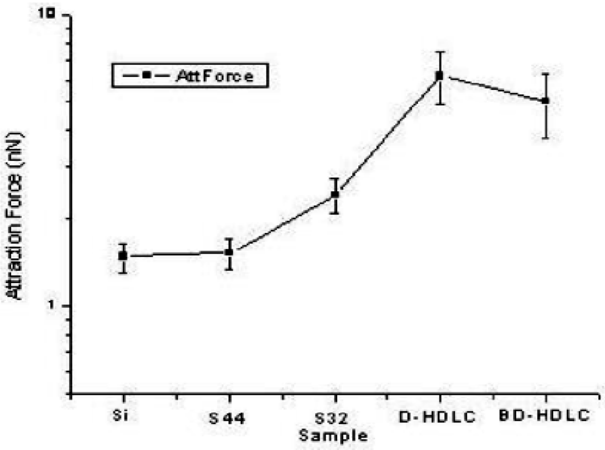

Fig. 8. Typical force of attraction vs of silicon surface (Si), HDLCs surface (S44 and S32), L-dopamine modified HDLC surface and BSA modified HDLC samples respectively.

Conclusion

Here we have presented a brief report on how roughness, continuity and force of attraction affected by the flow rates of H_2 and CH_4 during synthesis of HDLC films. From these results one can detect and predict the hydrogen dendity on the HDLC surfaces and also one can predict the presence of biomolecules onto the HDLC surfaces. Novel properties leading to useful application in the area of surface chemistry for future research and development tricks throughout the world.

Acknowledgements

The author (HSB) thanks University Grants Commission Reference No. F.PSW-140/15-16 (dated 15 Nov-2016), Govt. of India for funding during XII plan period for carrying out the present work. We thank Mr. Abir Ghosh, Mr. Subhasis Bala for their fruitful scientific discussions and Dr. S. Chattopadhyay and Dr. S. Bhuia, Dr. S. Chatterjee, Dr. L. Das for technical help.

References

1. H. S. Biswas, J. Datta, D. P. Chowdhury, A. V. R. Reddy, U. C. Ghosh, A. K. Srivastava and N. R. Ray, *Langmuir*, 2010, **26(22)**, 17413.
2. A. Singha, A. Ghosh, A. Roy and N. R. Ray, *J. Appl. Phys.*, 2006, **100**, 044910-1-8.
3. G. Binning, C. F. Quate and Ch. Gerber, *Phys. Rev. Lett.*, 1986, **56**, 930.
4. G. Binnig and H. Rohrer, *Helvetica Physica Acta*, 1982, **55**, 726.
5. Ioana Pera, Rüdiger Stark, Michael Kappl, Hans-Jürgen Butt and Fabio Benfenati, *Biophysical Journal*, 2004, **87**, 2446.
6. Eleonora Minelli, Gabriele Ciasca, Tanya Enny Sassun, Manila Antonelli, Valentina Palmieri, Massimiliano Papi, Giuseppe Maulucci, Antonio Santoro, Felice Giangaspero, Roberto Delfini, Gaetano Campi and Marco De Spirito, *Appl. Phys. Lett.*, 2017, **111**, 143701.
7. P. K. Hansma and J. Tersoff, *J. Appl. Phys.*, 1987, **2**, 61.
8. Simone Dinarelli, Marco Girasole and Giovanni Longo, *BMC Bioinformatics*, 2018, **19**, 258.
9. W. Lü, D. Yang, Y. Sun, Y. Guo, S. Xie and H. Li, *Applied Surface Science*, 1999, **147**, 39.
10. D. Wei, R. Dave and R. Pfeffer, *Journal of Nanoparticle Research*, 2002, **4**, 21.
11. Atsushi Ikai, Rehana Afrin and Hiroshi Sekiguchi, *Current Nanoscience,* 2007, **3**, 17.
12. Shiming Lin, Ji-Liang Chen, Long-Sun Huang and Huan-We Lin, *Current Proteomics,* 2005, **2**, 55.
13. A. Nancy, Burnham, Dawn D. Dominguez, Robert L. Mowery and Richard J. Colton, *Phys. Rev. Lett.*, 1990, **64**, 16.
14. Seung-woo Lee and Wolfgang M. Sigmund, *Colloids and Surfaces*, 2002, **204**, 43.
15. R. Zboril, M. Mashlan and D. Petridis, *Chemistry of Materials*, 2002, **14**, 969.